
Journal of Engineering Mathematics **50:** 121–140, 2004.

Subcritical and supercritical bifurcations of the first- and second-order Benney equations

ALEXANDER ORON and O. GOTTLIEB
*Department of Mechanical Engineering, Technion-Israel Institute of Technology, Haifa 32000, Israel, *Author for correspondence E-mail: meroron@tx.technion.ac.il*

Received 15 January 2004; accepted in revised form 25 June 2004

Abstract. The problem of the stability threshold of thin-film dynamics as described by the Benney equation of both first and second orders is revisited. The main result is that the primary Hopf bifurcation of the Benney equation of first order is supercritical for smaller values of Reynolds number and subcritical for its larger values. This result is numerically validated and further investigated analytically to reveal coexisting stable and unstable traveling waves. However, the primary bifurcation of the second-order Benney equation is supercritical for any Reynolds numbers. Sideband instability of traveling-wave regimes whose amplitude and frequency arise from the corresponding complex Ginzburg-Landau equation (CGLE) is found for the Benney equation of both first and second orders.

Key words: Benney equation, sideband instability, subcritical Hopf bifurcation, thin falling liquid films

1. Introduction

Falling liquid films are often encountered in various technological applications, such as evaporators, condensers, heat exchangers, coating, and physical phenomena, such as gravity currents and lava flows. The long-wave approach [1] has been found to be a useful tool of investigation in the case when the base state is a flow and the Reynolds number of the flow is *not* large. An example is the dynamics of a liquid film flow on a vertical or an inclined plane where the steady Nusselt flow is known to be unstable to small long-wave disturbances. The Nusselt flow undergoes a Hopf bifurcation which evolves to a variety of patterns, where the final pattern selection depends on the flow parameters.

In the pioneering work on this topic, Benney [2] derived the nonlinear partial differential evolution equation referred to nowadays as the Benney equation (BE). This evolution equation describes the nonlinear dynamics of the interface of a two-dimensional liquid film flowing on a fixed vertical or inclined plane. The Benney equation has been extensively studied over several decades. Traveling-wave solutions were investigated using the method of projection onto a low-dimensional manifold spanned over several modes [3–5]. More complex traveling-wave structures for the Benney equation were also investigated [5]. These traveling-wave solutions were found to be simple solitary and multi-humped localized waves. It was claimed [5] that solitary wave patterns observed in [6] in their experiments represent just a superposition of different solitary waves. Three-dimensional extensions of the Benney equation were derived in [7] and [8]. Higher-order evolution equations, with respect to the small expansion parameter that constitutes the aspect ratio of the wave, were derived in [4, 9]. The first-order Benney equation was numerically investigated as a partial differential equation in [10–15].

However, along with the success of the Benney equation model to describe the dynamics of falling liquid films, there is a serious drawback. It turns out that there exists a subdomain in parameter space, where the Benney equation exhibits solutions whose amplitude grows without bound. In this case the Benney equation loses its physical relevance. The feature of solutions blow-up for the Benney equation was first reported in [10] and further studied in [13], where the valid range of the Benney equation was mapped in the appropriate parameter space. Salamon *et al.* [16] carried out the study of traveling waves on vertical falling films by solving directly the full *stationary* hydrodynamic equations along with the free-surface boundary conditions using the finite elements method and compared the solutions with those of the Benney equation written in the moving frame of reference. The latter demonstrated coexisting traveling waves below the spurious blow-up. After extensive numerical simulations of the BE, Oron and Gottlieb [14] conjectured that the larger traveling waves are unstable. Recently, Gottlieb and Oron[17] demonstrated via a low-order modal projection, that the larger amplitude traveling waves are indeed unstable and that the blow-up threshold represents a saddle-node bifurcation.

The existence of the blow-up property of the Benney equation led to several attempts to develop alternative approaches to the derivation of the pertinent evolution equations for the same physical problem. Ooshida [18] conjectured that the traditional longwave expansion is poorly convergent and suggested replacing it by a regularized longwave expansion based on Padé approximations. He identified the important parameter $\delta = RW^{-1/3}$ referred to as the rescaled Reynolds number. Its importance arises from the fact that in the drag-gravity domain $\delta \ll 1$ the inertia plays a perturbative role, while in the drag-inertia domain $\delta \gg 1$ the inertia is dominant. The blow-up of the BE solutions occurs in the drag-inertia domain[18]. Recently alternative approaches that avoid the blow-up in the model equations have been introduced [19–23]. These alternatives are refinements of the integral methods [6, 24].

Lin [25] carried out the bifurcation analysis of the first- and second-order Benney equations and found (as follows from his expression given for J_2 and in spite of the curve $J_2 = 0$ drawn in the incorrect location in Figure 1 there) that the primary bifurcation is always supercritical. He also found that the filtered wave satisfying the pertinent complex Ginzburg-Landau equation is sideband stable. However, our results presented below disagree with his results in several aspects. Nakaya [4] and later Chang [26] carried out the bifurcation analysis of the third-order Benney equation. Their main result was that the type of the primary bifurcation of the third-order BE is supercritical, similar to that of the second-order BE [25].

The plan of the paper is as follows: Section 2 is devoted to the basic properties of the second-order Benney equation. In Section 3 we carry out the bifurcation analysis for the primary instability and derive the complex Ginzburg-Landau equation (CGLE) for both first- and second-order Benney equations. Section 4 deals with sideband instability of the monochromatic waves satisfying the CGLE. Section 5 contains the results of numerical verification of our bifurcation analysis. Section 6 is devoted to an analytical investigation of the properties of the Benney equation based on its low-dimensional modal projection. Section 7 contains discussion and closing remarks.

2. Preliminaries

We begin with the second-order Benney equation in the form given by Lin [25]

$$h_t + A(h)h_x + \alpha[B(h)h_x + C(h)h_{xxx}]_x + \alpha^2[D(h)h_x^2 + E(h)h_{xx} + F(h)h_{xxxx}$$

$$+ G(h)h_x h_{xxx} + H(h)h_{xx}^2 + I(h)h_x^2 h_{xx}]_x + O(\alpha^3) = 0, \tag{1a}$$

where

$$\begin{aligned} A(h) &= 2h^2,\ B(h) = \frac{8R}{15}h^6,\ C(h) = \frac{2}{3}Sh^3, \\ D(h) &= \frac{1016}{315}R^2h^9 + \frac{14}{3}h^3,\ E(h) = \frac{32}{63}R^2h^{10} + 2h^4, \\ F(h) &= \frac{40}{63}RSh^7,\ G(h) = \frac{16}{3}RSh^6,\ H(h) = \frac{16}{5}RSh^6,\ I(h) = \frac{32}{5}RSh^5. \end{aligned} \tag{1b}$$

Here $h = h(x, t)$ represents the nondimensional film thickness depending on the dimensionless independent spatial and temporal variables x and t, respectively. Equation (1a) describes the spatiotemporal dynamics of the two-dimensional liquid film of a mean thickness d falling on a static vertical ($\cot\beta = 0$) plate, when the physical properties of the liquid, such as density ρ, kinematic viscosity ν, and surface tension σ are specified.

The system parameters include the fundamental gravity- and surface tension-related dimensionless parameters R, W, which are Reynolds and inverse capillary numbers, respectively, and the small aspect-ratio parameter α

$$R = \frac{gd^3}{2\nu^2},\ W = \frac{\sigma}{\rho g d^2},\ \alpha = \frac{2\pi d}{\lambda}. \tag{2}$$

The Reynolds and the rescaled inverse capillary numbers R and $S = \alpha^2 W$ [3], respectively, are assumed in what follows to be $O(1)$ as $\alpha \to 0$.

The space-time variables (x, t) represent the corresponding physical space-time variables stretched by a small parameter α, defined in Equation (2) by the ratio between the average film thickness d multiplied by 2π and the characteristic wavelength of the interfacial disturbances λ. This wavelength is chosen as the entire length of the system so that solution domain for Equation (1a) is $0 \le x \le 2\pi$. In what follows the flow is considered in the entire domain of $(-\infty, \infty)$ with a 2π-periodicity.

The linearized version of Equation (1a) around its trivial solution $h_0 \equiv 1$ reads in terms of a small disturbance of the flat film interface $u = h - 1$

$$u_t + A_1 u_x + \alpha(B_1 u_{xx} + C_1 u_{xxxx}) + \alpha^2(E_1 u_{xxx} + F_1 u_{xxxxx}) + O(\alpha^3) = 0, \tag{3}$$

where from here on $A_1 = A(h = 1)$, $B_1 = B(h = 1)$, etc., $A_1' \equiv A'(h = 1)$, $B_1' \equiv B'(h = 1)$, $C_1' \equiv C'(h = 1)$, etc., $A_1'' \equiv A''(h = 1)$, $B_1'' \equiv B''(h = 1)$, $C_1'' \equiv C''(h = 1)$, etc., and primes denote differentiation with respect to h.

To order $O(\alpha^2)$, Equation (3) has a traveling-wave (TW) solution with the fundamental wavenumber $k_0 = 1$ in the form

$$u(x, t) = \Gamma \exp[\mathrm{i}(x - ct)] + \bar{\Gamma} \exp[-\mathrm{i}(x - \bar{c}t)], \tag{4}$$

where Γ is a complex amplitude of the wave independent of x, t, c is the complex wave celerity given by

$$c = c_r + \mathrm{i}c_i,\ c_r = A_1 - \alpha^2(E_1 - F_1),\ c_i = \alpha(B_1 - C_1), \tag{5}$$

and bars denote complex conjugates.

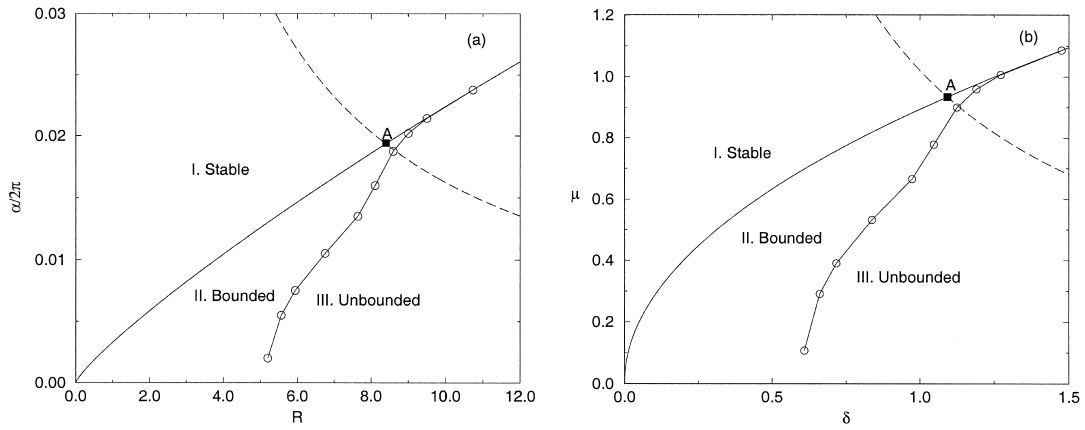

Figure 1. The stability diagram computed for thin water films, as described by Equation (7). It represents a different projection of the diagram found by Rosenau, Oron and Hyman [13]. The solid curve represents the linear stability threshold of the system. The curve marked by circles corresponds to the boundary between the domains of bounded and unbounded solutions for the BE1 computed numerically. The computations were not pursued for $\alpha/2\pi < 0{\cdot}002$ due to numerical complications. The intersection of the dashed and solid lines (A) represents the boundary between the supercritical and subcritical bifurcations located to its left and right, respectively. Thus, for $R < R(A)$ the bifurcation is supercritical, while for $R > R(A)$ the bifurcation is subcritical.

The solution $h = 1$ of the BE in the periodic domain $(0, 2\pi)$ is asymptotically stable (unstable) if $c_i < 0$ ($c_i > 0$), which is equivalent to $B_1 < C_1$ ($B_1 > C_1$). The onset of instability is oscillatory via a Hopf bifurcation. At the instability threshold of the system $B_1 = C_1$ the parameters of the problem are linked by the relationship

$$\alpha = \alpha_H \equiv (\frac{4R}{5W})^{1/2}. \tag{6a}$$

Beyond the threshold, the film surface evolves as a stationary wave propagating downstream with the speed c_r. Equation (6a) can be rewritten as

$$\alpha = \alpha_H \equiv (\frac{2^{5/6}}{\sqrt{5}})\frac{R^{4/3}}{\kappa^{1/2}} \tag{6b}$$

in terms of the Kapitza number

$$\kappa = \frac{\sigma}{\rho\nu^{4/3}g^{1/3}} \tag{6c}$$

that contains only the material properties of the liquid.

Figure 1(a) displays the stability diagram for a water film ($\nu = 1{\cdot}12 \times 10^{-2}$ cm^2/s, $\rho = 0{\cdot}999$ g/cm^3 and $\sigma = 73{\cdot}49$ dyn/cm [27]) in the $(\alpha - R)$ plane. The solid curve in Figure 1 represents the linear stability threshold of the system. The stability structure of the first-order Benney equation (BE1)

$$h_t + A(h)h_x + \alpha[B(h)h_x + C(h)h_{xxx}]_x + O(\alpha^2) = 0\ ,\ 0 \le x \le 2\pi, \tag{7}$$

was earlier investigated numerically in [13] and [14]. In accordance with the latters, the curve of the linear stability threshold of the system along with the curve marked by circles divide the plane into three regions: (I) linearly stable where small disturbances of the flat interface $h = 1$

decay and $h(t \to \infty) = 1$; (II) linearly unstable where the solutions of the BE1 are bounded for all times; (III) linearly unstable where the solutions of the BE1 grow with no saturation. These unbounded solutions are artifacts of the asymptotics related to long-wave expansions carried out in order to derive the evolution equation. Such unbounded solutions of the BE1 were first discovered numerically in [10] and were later classified and discussed in [13] and [14], who found the stability structure of the BE1 to include these three regions. Regions I and II are separated by the curve given by the Hopf stability criterion, Equation (6a), while regions II and III are separated by numerically obtained threshold for unbounded solutions [14].

3. Weakly nonlinear stability analysis of the Benney equation

Following as closely as possible the notation of Lin [25], we derive the Complex Ginzburg-Landau equation arising from the Benney equation (1a). In the vicinity of criticality given by $c_i = O(\varepsilon^2)$ which is equivalent to

$$B_1 - C_1 = O(\varepsilon^2) \ \text{ or } \ S = \frac{4}{5}R + O(\varepsilon^2), \tag{8}$$

the critical wavenumber is $k = 1$, the slow independent variables are defined by

$$X = \varepsilon x, \ T_1 = \varepsilon t, \ T_2 = \varepsilon^2 t, \tag{9}$$

where ε measures the distance from criticality, and the solution of (1a) is expanded in power series of ε as

$$h(\alpha, x, t, X, T_1, T_2) \equiv 1 + \varepsilon\eta(\alpha, x, t, X, T_1, T_2) = 1 + \varepsilon\eta_1 + \varepsilon^2\eta_2 + \varepsilon^3\eta_3 + \cdots \tag{10}$$

with $\eta_j = \eta_j(\alpha, x, t, X, T_1, T_2)$, $j = 1, 2, 3\cdots$.

Substituting Equations (9),(10) in (1a) yields

$$(L_0 + \varepsilon L_1 + \varepsilon^2 L_2 + \cdots)(\varepsilon\eta_1 + \varepsilon^2\eta_2 + \varepsilon^3\eta_3 + \cdots) = \text{nonlinear terms}, \tag{11}$$

where

$$\begin{aligned}
L_0 &= \frac{\partial}{\partial t} + A_1\frac{\partial}{\partial x} + \alpha(B_1\frac{\partial^2}{\partial x^2} + C_1\frac{\partial^4}{\partial x^4}) + \alpha^2(E_1\frac{\partial^3}{\partial x^3} + F_1\frac{\partial^5}{\partial x^5}),\\
L_1 &= \frac{\partial}{\partial T_1} + \frac{\partial}{\partial X}\left[A_1 + 2\alpha(B_1\frac{\partial}{\partial x} + 2C_1\frac{\partial^3}{\partial x^3}) + \alpha^2(3E_1\frac{\partial^2}{\partial x^2} + 5F_1\frac{\partial^4}{\partial x^4})\right],\\
L_2 &= \frac{\partial}{\partial T_2} + \frac{\partial^2}{\partial X^2}\left[\alpha(B_1 + 6C_1\frac{\partial^2}{\partial x^2}) + \alpha^2(3E_1\frac{\partial}{\partial x} + 10F_1\frac{\partial^3}{\partial x^3})\right].
\end{aligned} \tag{12}$$

At first order in ε one obtains from (1a)

$$L_0\eta_1 = 0, \tag{13}$$

which yields

$$\eta_1 = \Gamma \exp[\mathrm{i}(x - c_r t)] + \bar{\Gamma} \exp[-\mathrm{i}(x - c_r t)], \tag{14}$$

where the amplitude $\Gamma = \Gamma(X, T_1, T_2)$ is to be determined and c_r is given by (5).

At second order in ε one obtains from (1a) and (14)

$$L_0\eta_2 = -\left(\frac{\partial}{\partial T_1} + H_2\frac{\partial}{\partial X}\right)\Gamma \exp\left[\mathrm{i}(x - c_r t)\right] + Q_1\Gamma^2 \exp\left[2\mathrm{i}(x - c_r t)\right] + c.c., \tag{15}$$

where $c.c.$ denotes complex conjugate,

$$\begin{aligned} H_2 &\equiv H_{2r} + \mathrm{i}H_{2i} = A_1 - \alpha^2(3E_1 - 5F_1) + 2\mathrm{i}\alpha(B_1 - 2C_1), \\ Q_1 &= -\mathrm{i}A_1' + 2[\alpha(B_1' - C_1') + \mathrm{i}\alpha^2(D_1 + E_1' - F_1' - G_1 - H_1)], \end{aligned} \tag{16}$$

which coincides with the results of Lin [25], see Equation (17) there. Consequently, the function Γ has the functional form of $\Gamma = \Gamma(X - H_{2r}T_1, T_2)$, provided that $H_{2i} = O(\varepsilon)$.

Upon elimination of secular terms from (15) the solution is obtained as

$$\eta_2 = \tilde{H}_1\Gamma^2 \exp\left[2\mathrm{i}(x - c_r t)\right] + c.c., \tag{17}$$

where

$$\tilde{H}_1 \equiv \tilde{H}_{1r} + \mathrm{i}\tilde{H}_{1i} = \frac{Q_1}{2\alpha[2(4C_1 - B_1) + 3\mathrm{i}\alpha(5F_1 - E_1)]}, \tag{18}$$

which is different from what Lin obtained in his expression for H_1.

Substituting (14) and (17) in the equation obtained at third order in ε and eliminating its secular solution, we obtain using MATHEMATICA the following equation related to the complex Ginzburg-Landau equation (CGLE) for the perturbation amplitude Γ:

$$\frac{\partial\Gamma}{\partial T_2} + \mathrm{i}\mathrm{v}\frac{\partial\Gamma}{\partial X} - c_i'\Gamma + (J_{1r} + \mathrm{i}J_{1i})\frac{\partial^2\Gamma}{\partial X^2} + (J_2 + \mathrm{i}J_4)|\Gamma|^2\Gamma = 0, \tag{19}$$

where

$$c_i' = \varepsilon^{-2}c_i,\ \mathrm{v} = 2\alpha(2C_1 - B_1)\varepsilon^{-1} > 0, \tag{20a}$$

$$J_{1r} = \alpha(B_1 - 6C_1),\ J_{1i} = \alpha^2(3E_1 - 10F_1), \tag{20b}$$

$$J_2 = -A_1'\tilde{H}_{1i} + \alpha[\frac{1}{2}(C_1'' - B_1'') + (7C_1' - B_1')\tilde{H}_{1r}] + \alpha^2\tilde{H}_{1i}Z, \tag{20c}$$

$$\begin{aligned} J_4 = {} & A_1'\tilde{H}_{1r} + \frac{1}{2}A_1'' + \alpha\tilde{H}_{1i}(7C_1' - B_1') \\ & + \alpha^2[D_1' - \frac{3}{2}(E_1'' - F_1'') - G_1' + 3H_1' - I_1' - Z\tilde{H}_{1r}], \end{aligned} \tag{20d}$$

where

$$Z = -4D_1 + 5E_1' - 17F_1' + 10G_1 - 8H_1. \tag{20e}$$

Equation (19) is similar in its form to (18) obtained in [25] but differs from it in several aspects: (i) the coefficient of the diffusion term is not real as in [25], but has also an imaginary component $O(\alpha^2)$; (ii) the coefficients J_2 and J_4 now contain $O(\alpha^2)$-corrections consistently with the presence of $O(\alpha^2)$ terms in the second-order Benney equation; (iii) the wrong expression for H_1 given in [25] is now corrected in (18) and the wrong factor '10' that appears in the coefficients J_2 and J_4 given in [25, Equation (18)] is now corrected to '7' in (20) in the appropriate places; (iv) Equation (19) now contains an imaginary, apparently 'convective' v-term missing in [25].

It is instructive to note that Equation (19) can be reduced by transformation

$$\Gamma(X, T_2) = \exp(\mathrm{i}qX)\gamma(X, T_2),\ q = -\frac{\mathrm{v}}{2(J_{1r} + \mathrm{i}J_{1i})} \tag{21}$$

into the standard CGLE in the form

$$\frac{\partial\gamma}{\partial T_2} - [c_i' - \frac{\mathrm{v}^2}{4(J_{1r} + iJ_{1i})}]\gamma + (J_{1r} + iJ_{1i})\frac{\partial^2\gamma}{\partial X^2} + (J_2 + iJ_4)|\gamma|^2\gamma = 0, \tag{22}$$

where the coefficient of the linear, spatially homogeneous term now becomes complex.

The linear stability properties of the trivial solution $\Gamma = 0$ of (19) are now briefly outlined. Linearizing (19) about $\Gamma = 0$ and introducing the normal perturbation in the form const $\times \exp(\omega T_2 + \mathrm{i}kX)$ with complex growth rate ω and wavenumber k, both dimensionless, one arrives at the dispersion relation

$$\omega = c_i' + k\mathrm{v} + (J_{1r} + \mathrm{i}J_{1i})k^2. \tag{23}$$

Therefore, the disturbance will grow in time rendering by this the state $\Gamma = 0$ to be linearly unstable, if

$$\mathfrak{Re}(\omega) = c_i' + k\mathrm{v} + J_{1r}k^2 > 0. \tag{24}$$

This criterion is valid for longwave disturbances of

$$k < k_0 \equiv \frac{2c_i'}{\sqrt{\mathrm{v}^2 - 4J_{1r}c_i'} - \mathrm{v}} \tag{25}$$

for $c_i' > 0$, and in the interval

$$k_2 < k < k_1,\ k_2 = \frac{-2c_i'}{\mathrm{v} + \sqrt{\mathrm{v}^2 - 4J_{1r}c_i'}},\ k_1 = \frac{-2c_i'}{\mathrm{v} - \sqrt{\mathrm{v}^2 - 4J_{1r}c_i'}} \tag{26}$$

for $c_i' < 0$.

The character of the perturbation dynamics beyond the linear regime depends solely on the sign of J_2. When J_2 is positive, the saturation of the amplitude Γ is ensured. This is the case of a supercritical (forward) bifurcation. When J_2 is negative, the saturation does not occur (if higher-order terms in Γ are not accounted for), and the corresponding case is that of a subcritical (inverted) bifurcation.

3.1. BE1

In the case of the BE1 $D(h) = E(h) = F(h) = G(h) = H(h) = I(h) = 0$ (20) reduce to

$$c_i' = \varepsilon^{-2}c_i,\ \mathrm{v} = 2\alpha(2C_1 - B_1)\varepsilon^{-1}, \tag{27a}$$

$$J_{1r} = \alpha(B_1 - 6C_1),\ J_{1i} = 0, \tag{27b}$$

$$J_2 = -A_1'\tilde{H}_{1i} + \alpha[\frac{1}{2}(C_1'' - B_1'') + (7C_1' - B_1')\tilde{H}_{1r}], \tag{27c}$$

$$J_4 = A_1'\tilde{H}_{1r} + \frac{1}{2}A_1'' + \alpha\tilde{H}_{1i}(7C_1' - B_1'), \tag{27d}$$

where

$$\tilde{H}_1 \equiv \tilde{H}_{1r} + i\tilde{H}_{1i} = \frac{-iA_1' + 2\alpha(B_1' - C_1')}{4\alpha(4C_1 - B_1)}. \tag{27e}$$

Substitution of the corresponding values of the variables in (27) yields

$$J_{1r} = \alpha(B_1 - C_1) = -\frac{8\alpha R}{3},\ J_2 = \frac{5}{2\alpha R} - \frac{12\alpha R}{5},\ J_4 = -1. \tag{28}$$

In view of the fact that the first-order Benney equation is being considered, one may be puzzled by the result obtained for J_2, as given by (28), due to the emergence of powers of α differing by two. However, the same result containing two terms of different signs is obtained when the first-order equation, Equation (1a) with $D(h) = E(h) = F(h) = G(h) = H(h) = I(h) = 0$ is transformed by

$$h \to \alpha^{-2/11}h,\ x \to \alpha^{3/11}x,\ t \to \alpha^{7/11}t, \tag{29}$$

into the equation devoid of parameter α

$$h_t + 2h^2h_x + \frac{8R}{15}(h^6h_x)_x + \frac{2}{3}S(h^3h_{xxx})_x = 0. \tag{30}$$

The validity of this result will be numerically tested and verified in Section 5. Note that (30) reveals that the boundary-value problem at hand is governed by two system parameters. Note also that it is impossible to scale out the parameter α from the second-order Benney equation.

Therefore, the bifurcation as predicted by the first-order Benney equation is supercritical ($J_2 > 0$) if

$$R < R_c = \frac{5}{2\sqrt{6}\alpha}. \tag{31a}$$

For $R > R_c$

$$R > R_c = \frac{5}{2\sqrt{6}\alpha} \tag{31b}$$

the bifurcation is subcritical.

The dashed curve in Figure 1(a) given by (31) and corresponding to $J_2 = 0$ intersects with the Hopf curve given either by (6a) or by (6b) at the point A. Solving simultaneously (6a) with $J_2 = 0$ yields

$$R = R_c = \frac{5}{2 \cdot 12^{1/3}}W^{1/3} \approx 1{\cdot}092W^{1/3}, \tag{32a}$$

which is suitable in the general case. However, if the liquid is specified and its Kapitza number, Equation (6c), is prescribed, the appropriate expression for the critical value of the Reynolds number R_c is found from solving simultaneously (6b) and $J_2 = 0$

$$R = R_c = \frac{5^{9/11}}{2^{10/11} \cdot 3^{3/11}}\kappa^{3/11} \approx 1{\cdot}473\kappa^{3/11}. \tag{32b}$$

As follows from (31), the domain of supercritical bifurcation is located along the Hopf curve for $0 < R < R_c = R(A)$, and is subcritical for $R > R(A)$. This result will be verified both numerically and theoretically in Sections 5 and 6, respectively. In the case of water films, for instance, $R_c \approx 8{\cdot}3894$.

It should be noted here that the critical value of R_c from (31) is $O(\alpha^{-1})$, This is formally outside the asymptotic range of $R = O(1)$ for which the BE was systematically derived from

the Navier-Stokes equations. However, it represents a characteristics of the BE1 and can be verified in Figure 1 to be within the bounds of region II for a water film. Furthermore, this relation between the subcritical threshold and the blow-up of BE1 is not guaranteed as the transition between regions II and III is obtained numerically and we cannot rule out that the subcritical domain will appear beyond the critical value of R of the region III. We address this issue in Section 6.

Ooshida [18] found that the rescaled Reynolds number

$$\delta = \frac{R}{W^{1/3}}, \tag{33}$$

that appeared as a single parameter in the integral boundary-value equations [24, 19, 20], is very important because it naturally separates between two domains: the domain $\delta \ll 1$ where the inertia plays a perturbative role with respect to viscous effects (drag-gravity regime), and the domain $\delta \gg 1$ where inertia dominates the latter (drag-inertia regime). He also pointed out that the transition point between the two regimes is close to $\delta = 1$, and noted that beyond this value the long-wave Benney equation is invalid. Thus, Equation (7) can be recast into a single-fluid-parameter version in the form

$$h_t + 2h^2 h_x + \frac{8}{15}\delta\mu(h^6 h_x)_x + \frac{2}{3}\mu^3(h^3 h_{xxx})_x = 0, \tag{34}$$

where $\mu = \alpha W^{1/3}$. Note that under the fundamental assumption $S = \alpha^2 W = O(1)$, see Section 2, the revised perturbation parameter $\mu = \alpha W^{1/3}$ is $O(\alpha^{1/3})$. The film evolution governed by (34) and the linear stability threshold of the system in a finite periodic domain which can be written in similar to (6a) as

$$\mu = \mu_H = \left(\frac{4}{5}\delta\right)^{1/2},$$

depend on *both* δ and μ.

As seen in Figure 1(b) the transition between bounded and unbounded solutions of BE1 takes place in the range $0{\cdot}6 < \delta < 1{\cdot}5$. Furthermore, as seen from (32a) and from Figure 1(b), the point A that represents a *universal* transition from supercritical to subcritical bifurcation, $\delta = \delta_c \approx 1.092$, lies in the same neighborhood, as the limiting range of BE1.

Equation (34) is the BE1 written in the form where a single fluid parameter δ appears instead of two fluid parameters R, S in (7), along with a revised perturbation parameter μ. Note that if the fluid is specified, the two parameters R and S in (7) depend only on the mean film thickness d, thus effectively reducing the number of independent fluid parameters to one. When comparing between (7) and (34) one should bear in mind that the perturbation parameter, namely $\alpha = 2\pi d/\lambda$ and $\mu = \alpha W^{1/3}$, respectively, is *not* the same in both versions of the BE1. However, Equation (34) implies that the film dynamics is universal for all fluids, when analyzed in the $\delta - \mu$ parameter space [28].

Except for work of Lin [25], Nakaya [4] and Chang [26] also carried out the bifurcation analysis of the Benney equation of various orders. Nakaya [4] derived the expression for the Landau coefficient ($s_3 + \mathrm{i}\omega_3$ in his notation, see (45) there) in terms of the coefficients of the Benney equation R, W, the angle of inclination and the small expansion parameter μ that is equivalent to our coefficient α. The sign of s_3 determines there the type of the bifurcation. At the last stage of the derivation only the leading-order term with respect to μ proportional

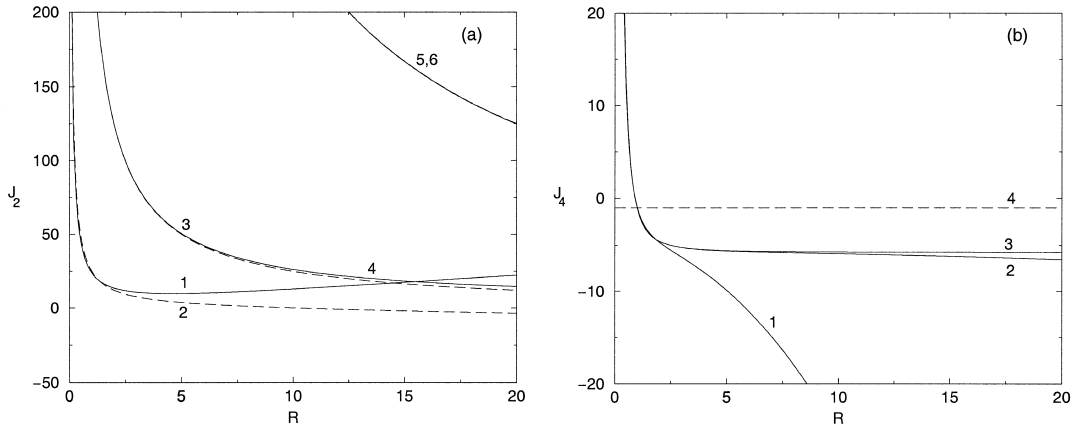

Figure 2. Variation of the coefficients J_2 and J_4 of Equation (19) with the Reynolds number R for various values of α. The broken and solid curves correspond to the first- and second-order Benney equations, respectively: (a) $\alpha = 0{\cdot}1$- curves 1, 2; $\alpha = 0{\cdot}01$- curves 3, 4; $\alpha = 0{\cdot}001$- curves 5, 6. (b) Curves 1, 2 and 3 correspond to $\alpha = 0{\cdot}1$, $0{\cdot}01$ and $0{\cdot}001$, respectively.

to $\mu^{-1}R^{-1}$ was retained in s_3. His result then is similar (but not identical, probably due to some algebraic errors in his derivations) to the first term in J_2 given in (28). We checked his result, taking into consideration the next term of the expansion of s_3 into series of μ. The conclusion is that he also would have obtained a term differing from the leading-order term by its sign and proportional to μ, similar to (28). It follows, therefore, that Nakaya [4] could have also obtained the transition from supercriticality to subcriticality similar to the results presented in this paper. The derivations of Chang [26] are based on setting $\mu = 1$ and on the scaling where the existence of the originally second-order in μ terms (at least one of them denoted there by $B(h)$ and B_0) is crucial, see his parameter ξ. The result with respect to the type of bifurcation obtained by Chang [26] is consistent with that of Lin [25] and with our own presented in the next subsection in the context of the second-order Benney equation. We note here that [31, 32] found the same transition from supercritical to subcritical bifurcation numerically using AUTO for stationary waves described by the BE1.

3.2. BE2

In the case of the second-order Benney equation (BE2) one obtains the following values for the coefficients of Equation (19)

$$J_{1i} = \alpha^2(6 - \frac{32}{9}R^2), \tag{35a}$$

$$J_2 = \frac{5}{2\alpha R} + \alpha(-\frac{1125}{128R^3} - \frac{955}{168R} + \frac{3338R}{2205}), \tag{35b}$$

$$J_4 = -\frac{121}{21} + \frac{75}{16R^2} + \alpha^2(\frac{43511}{1764} - \frac{16875}{1024R^4} + \frac{2725}{448R^2} + \frac{19948R^2}{46305}), \tag{35c}$$

where c_i', v, J_{1r} remain the same as in (27).

From inspection of Figure 2(a) displaying the variation of J_2 with α, R one finds that the curves corresponding to the BE2 bifurcate from those corresponding to the BE1 at a certain value of R. Note that curve 5 also deviates from curve 6 at large R, where the BE loses its validity. It follows from Figure 2(a) that J_2, as given by (35) for the BE2 is positive, rendering

its primary bifurcation supercritical. In this case our result agrees qualitatively with that of Lin [25].

As seen from Figure 2(b), displaying the variation of J_4 with α and R, the curves corresponding to the BE2 intersect that of BE1. This follows from the $O(1)$-correction to the value of J_4 given by (27) that arises from the first and third terms of (20). The result signals that the second-order BE does not represent a uniform extension of the first-order BE. This indicates that the convergence of the asymptotic series leading to the Benney equations is questionable as already suggested in [18]. In this context, if the second-order BE were an $O(\alpha^2)$- correction of the first-order BE, an order-one correction for J_4 would not arise. On the other hand, the curves corresponding to the second-order BE and different values of α smoothly bifurcate from each other at a certain value of R.

One can notice that both J_2 and J_4, as presented by (35) undergo a fast variation and change their sign at $R \to 0$, but in this domain the asymptotic expansions presented here will not be valid, as R would not be $O(1)$ there, but represented by some power of α.

4. Sideband instability of the spatially uniform solution of CGLE

In this section we investigate stability of the spatially uniform solution of Equation (19) with respect to infinitesimal sideband disturbances. It is emphasized that spatially uniform solutions of (19) correspond to traveling-wave (TW) regimes, as described by the Benney equation (1a). The notation of Lin [25] will be followed as closely as possible. The following analysis is carried out for both the supercritical, $J_2 > 0, c_i' > 0$ and subcritical, $J_2 < 0, c_i' < 0$ cases. We reiterate here that according to the results of the previous section the bifurcation in the case of BE2 is always supercritical, while in the case of BE1 it is supercritical for smaller values of R and subcritical for larger values of R.

Seeking spatially uniform solutions of (19) in the exponential form $\Gamma_\infty(T_2) = |\Gamma_\infty| \exp(-\mathrm{i}QT_2)$ results in

$$Q = \frac{c_i' J_4}{J_2},\ |\Gamma_\infty|^2 = \frac{c_i'}{J_2}. \tag{36}$$

This solution is perturbed by small spatial sideband disturbances in the form

$$\Gamma = \Gamma_\infty(T_2) + [\delta\Gamma_+(T_2) \exp(\mathrm{i}KX) + \delta\Gamma_-(T_2) \exp(-\mathrm{i}KX)] \exp(-\mathrm{i}QT_2) \tag{37}$$

with K being the modulation wave number and it is substituted in (19). Neglecting the terms containing nonlinearities of $\delta\Gamma_+, \delta\Gamma_-$ one obtains

$$\frac{\partial}{\partial T_2}\begin{pmatrix}\delta\Gamma_+\\ \delta\bar{\Gamma}_-\end{pmatrix} = \mathbf{A}\begin{pmatrix}\delta\Gamma_+\\ \delta\bar{\Gamma}_-\end{pmatrix} \equiv \begin{pmatrix}A_{11} & A_{12}\\ A_{21} & A_{22}\end{pmatrix}\begin{pmatrix}\delta\Gamma_+\\ \delta\bar{\Gamma}_-\end{pmatrix}, \tag{38}$$

where

$$\begin{aligned} A_{11} &= -2(J_2 + \mathrm{i}J_4)|\Gamma_\infty|^2 + \mathrm{i}Q + c_i' + (J_{1r} + \mathrm{i}J_{1i})K^2 + K\mathrm{v},\\ A_{22} &= -2(J_2 - \mathrm{i}J_4)|\Gamma_\infty|^2 - \mathrm{i}Q + c_i' + (J_{1r} - \mathrm{i}J_{1i})K^2 - K\mathrm{v},\\ A_{12} &= -(J_2 + \mathrm{i}J_4)|\Gamma_\infty|^2,\ A_{21} = \bar{A}_{12}. \end{aligned} \tag{39}$$

Seeking solutions of (38) in the form

$$\begin{pmatrix}\delta\Gamma_+\\ \delta\bar{\Gamma}_-\end{pmatrix} = \begin{pmatrix}c_+\\ c_-\end{pmatrix} \exp(\lambda T_2) \tag{40}$$

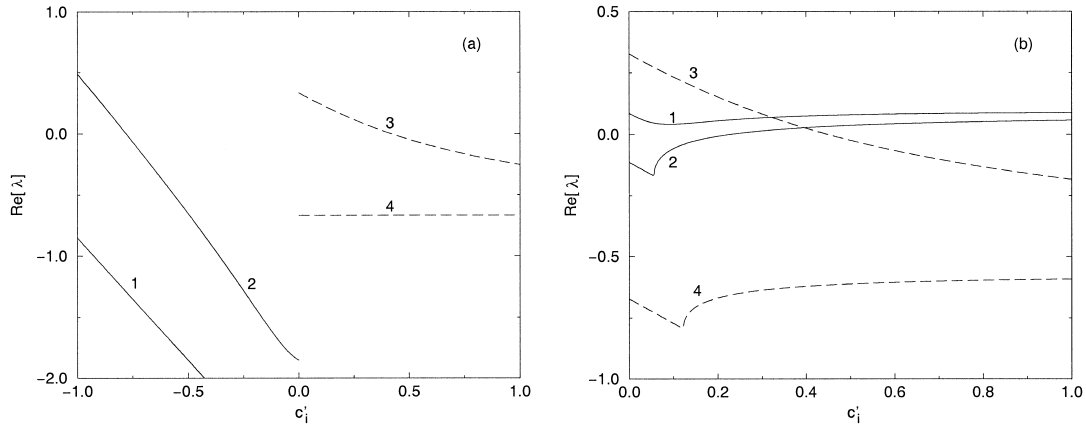

Figure 3. The largest real part of the eigenvalue λ_1 of matrix $\mathbf{A}$ for water films. (a) The first-order Benney equation: curves 1, 2 - $d = 1{\cdot}3 \times 10^{-2}$ cm, $\alpha = 0{\cdot}1245$, $K = 1$ with v $= 0$ and 1, respectively; curves 3, 4 - $d = 1{\cdot}0 \times 10^{-2}$ cm, $\alpha = 0{\cdot}0645$, $K = 1$ with v $= 1$ and 0, respectively. (b) The second-order Benney equation: curves 1, 2 - $d = 1{\cdot}3 \times 10^{-2}$ cm, $\alpha = 0{\cdot}1244$, $K = 0{\cdot}2$ with v $= 1$ and 0, respectively; curves 3, 4 - $d = 1{\cdot}0 \times 10^{-2}$ cm, $\alpha = 0{\cdot}0645$, $K = 1$ with v $= 1$ and 0, respectively.

results in two eigenvalues being the complex growth rate of the disturbance. It is readily seen that $\mathrm{tr}(\mathbf{A}) = A_{11} + A_{22}$ is real and negative for $c_i' > 0$, therefore at least one of the eigenvalues is in this case real and negative, which corresponds to the linearly sideband stable mode. The other eigenvalue can, however, have either positive or negative real part depending on the values of the problem parameters. In the former case the spatially uniform solution of CGLE is sideband unstable.

Equation (38) yields in the particular case of $J_{1i} = 0$, v $= 0$ considered in [25] two negative eigenvalues $\lambda_1 = J_{1r}K^2$, $\lambda_2 = J_{1r}K^2 - 2c_i'$. This implies that the spatially uniform solution of (19) is stable with respect to sideband disturbances for $c_i' > 0$ (the case considered there). This result is valid, according to our derivations in the case of the first-order Benney equation, as in this case $J_{1i} = 0$, if v is formally smaller than $O(\varepsilon)$, and thus neglected in (19).

In the particular case of v $= 0$, it is readily seen that $A_{22} = \bar{A}_{11}$, and therefore the determinant of $\mathbf{A}$ is real and

$$\det(\mathbf{A}) = (K^2 J_{1r} - 2c_i')K^2 J_{1r} + (K^2 J_{1i} - 2Q)K^2 J_{1i}. \tag{41}$$

The first-term of the right-hand side of (41) is always positive in the supercritical case $c_i' > 0$ and $K \neq 0$, while the second one can be of either sign. The spatially uniform solution of (19) given by (36) is thus sideband stable if $\det\mathbf{A} > 0$ and sideband unstable otherwise.

In the case of BE2 $J_{1i} \neq 0$ in general. Thus, sideband instability of the basic TW corresponding to (36) may emerge. Indeed the condition for the latter, $\det\mathbf{A} < 0$ implies

$$K^2 \leq K_{sb}^2 \equiv \frac{2c_i'}{|J_1|^2}(J_{1r} + \frac{J_4 J_{1i}}{J_2}). \tag{42}$$

It follows from (42) that in the supercritical case with v $= o(\varepsilon)$ sideband instability emerges when $J_{1r} + J_4 J_{1i}/J_2 > 0$, is a longwave one. The latter is the well-known condition for Benjamin-Feir instability [29, 30].

In the presence of the v-term in (19) the analysis seems to be less obvious and thus relies on direct computation of the eigenvalues of $\mathbf{A}$. It is found that the spatially uniform solution

of (19) given by (36) can become sideband unstable, even when perturbed with sideband disturbance of the same wavenumber $K = 1$. Figure 3a shows the largest real part of the eigenvalue that can change its sign (recall that the other one is always real and negative) in the case of BE1. Our computations are carried out for water films in both supercritical, *e.g.* $d = 1{\cdot}0 \times 10^{-2}$ cm, and subcritical, *e.g.* $d = 1{\cdot}3 \times 10^{-2}$ cm, domains (see Section 5), so that in both of them $c_i'/J_2 > 0$. The values of α were chosen to be adjacent to the respective values of the linear stability threshold α_H: $\alpha < \alpha_H$ in the supercritical case and $\alpha > \alpha_H$ in the subcritical one. In both cases one reveals that in agreement with the analysis given above, the basic TW is sideband stable for v = 0. It becomes, however, sideband unstable, as displayed in Figure 3a, when v = 1 for $|c_i'|$ exceeding a certain positive value in the subcritical case, and for all $0 < c_i' < 1$ in the supercritical one. Our numerical study shows that in general the range of c_i' corresponding to sideband instability of the basic TW expands, when the value of v increases from 0 to 1 with the disturbance wavenumber K remaining fixed, and when the wavelength of the disturbance increases when v is fixed.

In the case of BE2 only a supercritical bifurcation is possible (see Section 3), thus the domain of $c_i' > 0$ only is shown in Figure 3b. Again, the values of α are chosen to be next to α_H, this time only $\alpha < \alpha_H$, as the bifurcation is supercritical. In the case of BE2 the basic TW is found to be sideband stable for $d < 1{\cdot}3 \times 10^{-2}$ cm with v = 0 in the range of $0{\cdot}001 \leq K \leq 1$ and sideband unstable for $d \geq 1{\cdot}3 \times 10^{-2}$ cm with v = 0 for appropriate values of c_i'. Sideband instability is also found for $v \neq 0$. A similar trend of variation of the sideband unstable range of c_i' is found for BE2, as for BE1.

5. Numerical investigation of the first-order Benney equation

In order to carry out a validation of our results obtained in Section 3 for the weakly nonlinear dynamics of water films, as described by the first-order Benney equation, we use the relationship between d and α at the stability threshold obtained from (6a), and (31a), (31b). These yield that for $d < d_c$ the primary bifurcation is supercritical, while for $d > d_c$ it is subcritical, where

$$d_c = \left(\frac{5\sqrt{5}}{2\sqrt{3}} \cdot \frac{\nu^3 \sigma^{1/2}}{g^2 \rho^{1/2}} \right)^{2/11} . \tag{43}$$

The value of d_c given by (43) corresponds to $\delta = \delta_c \approx 1{\cdot}092$. Upon introduction of the physical properties of water into (43) we find that $d_c = 1{\cdot}28976 \times 10^{-2}$ cm.

Equation (7) is numerically solved along with periodic boundary conditions in the domain $0 \leq x \leq 2\pi$ and the coefficients $B(h), C(h)$ calculated for water films of varying thicknesses d ranging around the critical value of d_c given by (43). The results of such computations were recently presented in [14]. Both regimes of traveling stationary and nonstationary waves were found. Here we are concerned with numerical validation of our asymptotic analysis in the case of the primary bifurcation of BE1.

Figure 4 displays the variation of the wave amplitude represented by the normalized peak-to-peak size of the wave

$$\zeta = \frac{h_{\max} - h_{\min}}{h_{\max} + h_{\min}} \tag{44}$$

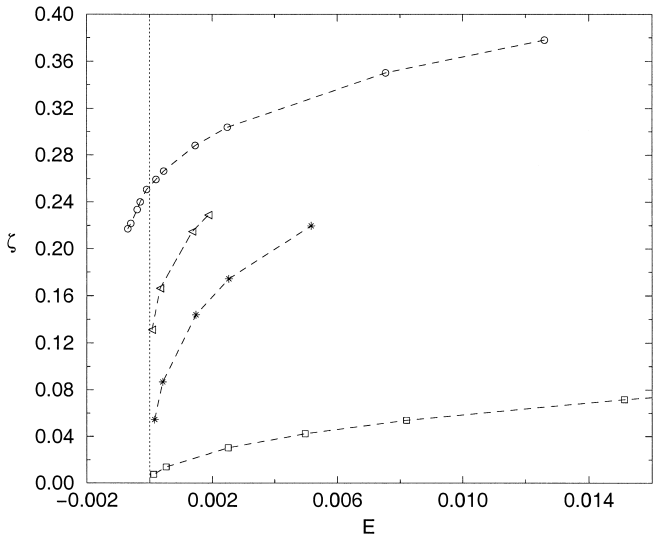

Figure 4. Variation of the wave amplitude, as computed from Equation (7) and expressed in terms of the parameter ζ, (44), with the distance from criticality, as expressed in terms of the parameter E, (45), for various values of the thickness of the water film: $d = 1{\cdot}1 \times 10^{-2}$cm ($\delta = 0{\cdot}609$) denoted by squares, $d = 1{\cdot}28 \times 10^{-2}$cm ($\delta = 1{\cdot}062$) denoted by stars, $d = 1{\cdot}292 \times 10^{-2}$cm ($\delta = 1{\cdot}099$) denoted by triangles, and $d = 1{\cdot}3 \times 10^{-2}$cm ($\delta = 1{\cdot}124$) denoted by circles. The dashed lines are drawn to guide the reader's eye. The vertical dotted line corresponds to the linear stability threshold, $E = 0$. The branch of the curve corresponding to $d = 1{\cdot}3 \times 10^{-2}$cm ($\delta = 1{\cdot}124$) that extends into the domain of negative E shows subcritical type of bifurcation in support of our theoretical predictions.

with the aspect ratio α, as presented in terms of the measure of the distance from criticality

$$E = \frac{\alpha_H - \alpha}{\alpha_H}, \tag{45}$$

where α_H is the critical value of α at the Hopf-stability threshold for the specified film thickness d.

Consistently with our theoretical predictions made in Section 3, the wave amplitude expressed by ζ tends to a nonzero value of $\zeta \approx 0{\cdot}259$ when $\alpha \to \alpha_H$ in the case of $d = 1{\cdot}3 \times 10^{-2}$cm ($\delta = 1{\cdot}124$). The branch of this curve that extends into the domain of negative E corresponding to $\alpha > \alpha_H$, which constitutes the linearly stable domain. This fact provides the numerical evidence of the subcritical solution and verification of the theoretical results, (31a),(31b). Furthermore, the results corresponding to $d = 1{\cdot}1 \times 10^{-2}$cm ($\delta = 0{\cdot}609$) are consistent with the predicted supercritical character of the primary bifurcation and the value of ζ decreases to zero with decreasing E ($\zeta \to 0$ as $\alpha \to \alpha_H$). The curve corresponding to $d = 1{\cdot}28 \times 10^{-2}$cm ($\delta = 1{\cdot}062$) represents a supercritical case according to (31a) and bends down in the vicinity of $E = 0$, as if it were pointing to the reference point of the graph. However, we note that one cannot numerically resolve the question whether it actually reaches the reference point. Thus, in order to further investigate the subcritical domain and its characteristics, we investigate a two-mode dynamical system. We note that the subcritical domain (located above the Hopf curve for $R > R(A)$) is particularly difficult to determine as numerical continuation methods are costly.

6. Stability analysis of a truncated bimodal dynamical system

In a recent paper Gottlieb and Oron [17] demonstrated the validity of a finite, low-order modal expansion with respect to the numerically solved BE1. Furthermore, a two-mode model was found to coincide with the numerical solution along the Hopf curve separating regions I and II.

Consider a solution of (7) in a truncated Fourier series

$$h(x,t) = 1 + \sum_{n=1}^{N} [z_n(t)\exp(\mathrm{i}nx) + \bar{z}_n(t)\exp(-\mathrm{i}nx)], \tag{46}$$

where $\bar{z}_n$ denotes the complex conjugate of z_n. Substitution of (46) into (7) and truncation to $N = 2$ yields

$$\begin{aligned} \dot{z}_1 &= [\mu_{111}z_1 + \mu_{121}\bar{z}_1 z_2 + z_1(\mu_{131}|z_1|^2 + \mu_{132}|z_2|^2)], \\ \dot{z}_2 &= [\mu_{211}z_2 + \mu_{221}z_1^2 + z_2(\mu_{231}|z_1|^2 + \mu_{232}|z_2|^2)], \end{aligned} \tag{47}$$

where the coefficients μ_{kji} are given by

$$\begin{aligned} \mu_{111} &= \alpha(B_1 - C_1) - 2\mathrm{i}, & \mu_{211} &= \alpha(4B_1 - 16C_1) - 4\mathrm{i}, \\ \mu_{121} &= \alpha(6B_1 - 21C_1) - 4\mathrm{i}, & \mu_{221} &= \alpha(12B_1 - 6C_1) - 4\mathrm{i}, \\ \mu_{131} &= \alpha(15B_1 - 3C_1) - 2\mathrm{i}, & \mu_{231} &= \alpha(120B_1 - 96C_1) - 8\mathrm{i}, \\ \mu_{132} &= \alpha(30B_1 - 6C_1) - 4\mathrm{i}, & \mu_{232} &= \alpha(60B_1 - 48C_1) - 4\mathrm{i}. \end{aligned} \tag{48}$$

The dynamical system (47) can be conveniently put in polar notation using $z_n = a_n \exp(\mathrm{i}\theta_n)$, and then be further reduced employing the phase relationship $\phi = 2\theta_1 - \theta_2$

$$\dot{a}_1 = \beta_{111}a_1 + (\beta_{121}\cos\phi - 4\sin\phi)a_1a_2 + a_1(\beta_{131}a_1^2 + \beta_{132}a_2^2), \tag{49a}$$

$$\dot{a}_2 = \beta_{211}a_2 + (\beta_{221}\cos\phi + 4\sin\phi)a_1^2 + a_2(\beta_{231}a_1^2 + \beta_{232}a_2^2), \tag{49b}$$

$$\dot{\phi} = (-2\beta_{121}\sin\phi - 8\cos\phi)a_2 + (-\beta_{221}\sin\phi + 4\cos\phi)\frac{a_1^2}{a_2} - 4(a_2^2 - a_1^2), \tag{49c}$$

where $\beta_{nji} = \mathfrak{Re}(\mu_{nji})$.

Traveling waves of the modal system (47) correspond to fixed points of the reduced polar equations (49) with a constant, nonzero phase difference ($\dot{a}_1 = \dot{a}_2 = \dot{\phi} = 0$). Close to the Hopf bifurcation we assume that the modal amplitudes are both small and ordered as $a_1 \to \varepsilon a_1,\ a_2 \to \varepsilon^2 a_2$. Consequently, the phase evolution is governed by the second term in the right-hand side of (49c).

Thus the phase component of the fixed point (ϕ^*) is given by

$$\tan\phi^* = \frac{4}{\beta_{221}} = \text{const} + O(\varepsilon^2). \tag{50}$$

Substitution of ϕ^* from (50) in (49a) results in an explicit expression for a_1^2

$$\beta_{131}a_1^2 = -(\beta_{111} + \kappa_1 a_2) \tag{51}$$

and a quadratic equation in terms of a_2 from (49b).

$$\kappa_1\beta_{231}a_2^2 + (\beta_{111}\beta_{231} - \beta_{131}\beta_{211} + \kappa_1\kappa_2)a_2 + \beta_{111}\kappa_2 = 0, \tag{52}$$

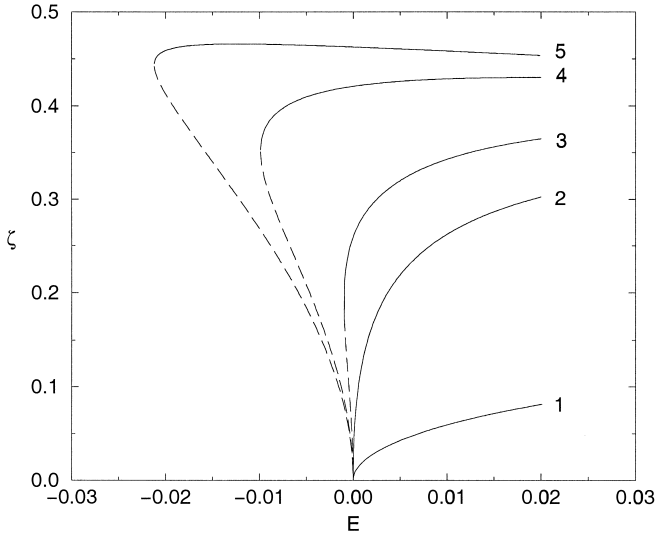

Figure 5. Variation of the wave amplitude, as expressed in terms of the parameter ζ, (44) with the distance from criticality, as expressed in terms of the parameter E, (45), for various values of the thickness of the water film, as computed using Equation (59). The solid curves correspond to stable solutions, while the dashed curves correspond to the unstable ones. Curve 1: $d = 1{\cdot}1 \times 10^{-2}$cm ($\delta = 0{\cdot}609$); 2: $d = 1{\cdot}28 \times 10^{-2}$cm ($\delta = 1{\cdot}062$); 3: $d = 1{\cdot}3 \times 10^{-2}$cm ($\delta = 1{\cdot}124$); 4: $d = 1{\cdot}32 \times 10^{-2}$cm ($\delta = 1{\cdot}189$); 5: $d = 1{\cdot}3275 \times 10^{-2}$cm ($\delta = 1{\cdot}214$).

where

$$\kappa_1 = \beta_{121}\cos\phi^* - 4\sin\phi^*, \kappa_2 = \beta_{221}\cos\phi^* + 4\sin\phi^*. \tag{53}$$

Recall that the Hopf bifurcation at the stability threshold is defined by $B_1 = C_1$ which is $\beta_{111} = 0$. Consequently, the amplitude of the nonzero traveling wave is given by

$$a_2 = \frac{\beta_{131}\beta_{211} - \kappa_1\kappa_2}{\beta_{231}\kappa_1}. \tag{54}$$

Note that a zero amplitude in (54) corresponds to the threshold for the subcritical TW. Thus, using

$$\beta_{131}\beta_{211} = \beta_{121}\beta_{221} - 16. \tag{55}$$

and substituting of β_{nji} in the zero value of a_2, as obtained from (54) yields

$$R = \frac{5}{2\sqrt{6}\alpha}, \tag{56}$$

which is identical to the criterion (31a) and (31b) derived above.

Figure 5 describes the variation of the normalized amplitude ζ, Equation (44), given for the bimodal system by

$$\zeta = 2\sqrt{a_1^2 + a_2^2}, \tag{57}$$

as a function of the normalized distance from criticality E, Equation (45).

Recall that a critical value of water film thickness is $d_c = 1{\cdot}28976 \times 10^{-2}$ cm ($\delta = 1{\cdot}092$). Note that for thickness below d_c, the normalized amplitude monotonically decreases to zero, as

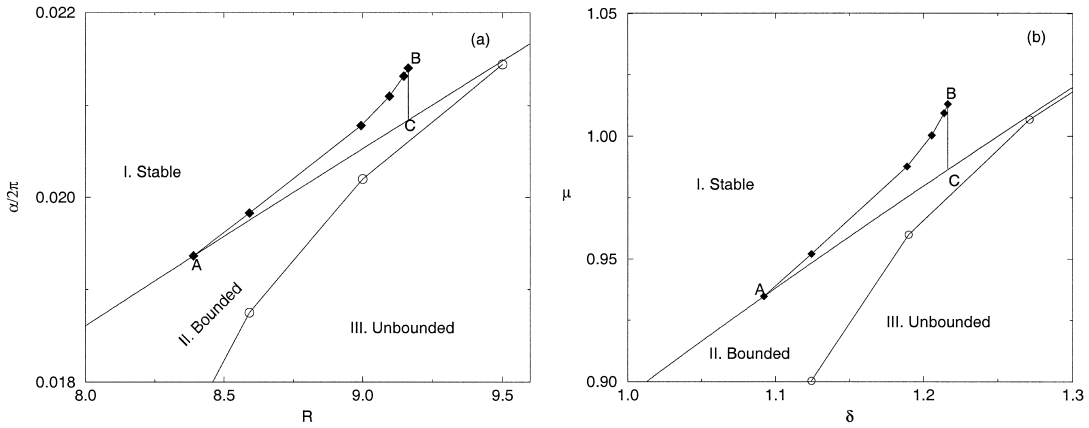

Figure 6. The subcritical stability diagram computed for thin water films, as described by (7). The solid line and the curve marked by circles are the same as in Figure 1, respectively. The curve marked by black diamonds and connecting points A and B, determines along with point C, the subcritical domain of coexisting traveling waves of Figure 5.

predicted by the supercritical character of the bifurcation. This is depicted by curves 1 and 2 in Figure 5 which are identical to the numerically obtained curves in Figure 4 for $d = 1{\cdot}1 \times 10^{-2}$ ($\delta = 0{\cdot}609$) and $1{\cdot}28 \times 10^{-2}$ cm ($\delta = 1{\cdot}062$), respectively. However, for values above d_c the solution decreases monotonically to the value given by (54). This is depicted by curves 3, 4, and 5 in Figure 5 corresponding to $d = 1{\cdot}3$, $1{\cdot}32$, $1{\cdot}3275 \times 10^{-2}$cm ($\delta = 1{\cdot}124$, $1{\cdot}189$, $1{\cdot}214$), respectively. We note that the solution of (52) with (50), (51) yields the predicted coexisting subcritical traveling wave solutions in region I for $E < 0$ ($\alpha > \alpha_H$). A comparison between curve 3 for $d = 1{\cdot}3 \times 10^{-2}$cm ($\delta = 1{\cdot}124$) and its numerical counterpart in Figure 4, reveals a slight discrepancy for a wave height greater than $\zeta \approx 0{\cdot}3$. The numerically obtained wave is slightly higher than that of the two-mode approximation ($\approx 8\%$ for $E \approx 0{\cdot}0125$).

The domain of existence of the subcritical traveling waves is delineated by the zero value of the discriminant of (52)

$$(\beta_{111}\beta_{231} - \beta_{131}\beta_{211} + \kappa_1\kappa_2)^2 - 4\beta_{111}\beta_{231}\kappa_1\kappa_2 = 0. \tag{58}$$

The solution of (58) is depicted by the curve connecting A and B in Figure 6. We note that beyond $R > R(B)$, no subcritical solution was found.

Stability of the subcritical TW is determined via the cubic eigenfunction deduced from the Jacobian of (49) calculated at the corresponding fixed points

$$\mathbf{J} = \begin{pmatrix} 2\beta_{131}a_1^2 & \kappa_1 a_1 & -a_1a_2(\beta_{121} + \beta_{221})\sin\phi \\ 2a_1(\kappa_2 + \beta_{231}a_2) & \beta_{211} + \beta_{231}a_1^2 & 0 \\ 8a_1 & -2(\beta_{121} + \beta_{221})\sin\phi & -\kappa_2 a_1^2 a_2^{-1} - 2\kappa_1 a_2 \end{pmatrix}. \tag{59}$$

The lower of the two TW yields a positive real eigenvalue corresponding to unstable saddle-foci denoted by dashed curves in Figure 5, whereas the upper TW have negative real parts and are stable sinks. Consequently, as anticipated, the bifurcation points defined by the zero discriminant are saddle- nodes.

Finally, we note that the closed subcritical domain in Figure 6 defined by points ABC may deform, because point B is deduced from a two-mode truncation which has been shown to be accurate near the Hopf transition but yields slightly lower values than those obtained

numerically from BE1 presented in Figure 4. Furthermore, we note that [31, 32] found a similar subcritical domain of TW in their investigation of traveling waves of BE1 using AUTO software for water films. However, while our numerically obtained curve denoted by circles in Figure 6, tends to the linear stability threshold curve from below, their curve for blow-up intersects the Hopf curve at $R \approx 8{\cdot}9$, and connects directly to their point B in region I.

7. Discussion and closing remarks

In this paper we have carried out the bifurcation analysis of the first- and second-order Benney equations. The main result of this analysis shows that the primary bifurcation of the first-order Benney equation is supercritical, when the Reynolds number is below a certain critical value, and is subcritical, when the Reynolds number exceeds the latter. However, the second-order Benney equation exhibits only a supercritical bifurcation.

The subcritical structure of BE1 was verified numerically and further investigated analytically by a two-mode dynamical system. This truncation accurately describes solutions near the transition from regions I and II and yields the exact transition to subcriticality. Furthermore, the analysis of Section 6 enables determination of a closed subdomain (within region I) describing coexisting TW predicted by the subcritical Hopf bifurcation. The upper/lower waves were found to be stable/unstable, respectively, and their transition to be defined by a saddle-node bifurcation.

The second-order Benney equation does not exhibit the subcritical bifurcation. This result may be an expression of a fact that was already attributed to the Benney equation in [18]: the asymptotic expansions leading to the derivation of the Benney equation may be poorly converging. A manifestation of the poor convergence of the asymptotic expansion scheme in the case at hand follows from the CGLE which has been derived in this paper. If the asymptotic procedure were converging at this stage, the coefficients of the CGLE would be expected to slightly change, as a result of going from the first-order to the second-order Benney equation. However, as shown here, the coefficients J_2 and especially J_4 significantly change between the subsequent orders of the Benney equation.

Sideband stability of the basic monochromatic traveling waves (TW) arising as the solutions of the CGLE has also been investigated in this paper. In contrast with the results obtained in [25] who claimed that these TW are sideband stable, we find that they may be sideband unstable depending primarily on the wavelength of a sideband disturbance and on the value of the coefficient of the 'convective' term in the corresponding CGLE, (19). This sideband instability can emerge in both supercritical and subcritical domains. Although we have not numerically solved both CGLE, (19), or BE2, we conjecture on the outcome of this sideband instability of the TW given by (36). As both blow-up of the corresponding TW and the emergence of a non-stationary wave in the close proximity to the linear stability threshold appear unlikely, the possibility of the emergence of a TW with a different amplitude, wavelength and celerity than in (36), may be a preferred option.

Acknowledgements

This research is partially supported by the Israel Science Foundation founded by the Israel Academy of Sciences and Humanities through Grant 369/99 and by the ICOPAC Research Network of the European Union (contract HPRN-CT-2000-00136). It is a pleasure to thank

Prof. A. A. Nepomnyashchy for illuminating discussions. The authors are indebted to Ms. E. Novbari, Mr. Y. Toledo and Dr. L. Yoffe for their assistance with the numerical simulations at different stages of this research. We thank the referees of the paper for their meaningful and constructive comments and suggestions that helped improve the quality of the paper. In particular, it is a pleasure to acknowledge stimulating discussions with Dr. Christian Ruyer-Quil with respect to universality of the results in the $\delta - \mu$ parameter plane.

References

1. A. Oron, S.H. Davis and S.G. Bankoff, Long-scale evolution of thin liquid films. *Rev. Mod. Phys.* 69 (1997) 931–980.
2. D.J. Benney, Long waves on liquid films. *J. Math. Phys.* 45 (1966) 150–155.
3. B. Gjevik, Occurrence of finite-amplitude surface waves on falling liquid films. *Phys. Fluids* 13 (1970) 1918–1925.
4. C. Nakaya, Long waves on a thin fluid layer flowing down an inclined plane. *Phys. Fluids* 15 (1975) 1407–1412.
5. C. Nakaya, Waves on a viscous fluid film down a vertical wall. *Phys. Fluids A* 1 (1989) 1143–1154.
6. P.L. Kapitza and S.P. Kapitza, Wave flow of thin layers of a viscous fluid. *Zh. Eksper. i Teor. Fiz.* 19 (1949) 105–120. Also, In: D. ter Haar (ed.), *Collected Papers.* Oxford: Pergamon Press (1965) pp. 690–709.
7. G.J. Roskes, Three-dimensional long waves on a liquid film. *Phys. Fluids* 13 (1970) 1440–1445.
8. M.V.G. Krishna and S.P. Lin, Stability of a liquid film with respect to initially finite three-dimensional disturbances. *Phys. Fluids* 20 (1977) 1039–1044.
9. B. Gjevik, Spatially varying finite-amplitude wave trains on falling liquid films. *Acta Polytech. Scand. Mech. Engng.* 61 (1971) 1–16.
10. A. Pumir, P. Manneville and Y. Pomeau, On solitary waves running down an inclined plane. *J. Fluid Mech.* 135 (1983) 27–50.
11. S.W. Joo, S.H. Davis and S.G. Bankoff, Long-wave instabilities of heated falling films: two-dimensional theory of uniform layers. *J. Fluid Mech.* 230 (1991) 117–146.
12. S.W. Joo and S.H. Davis, Instabilities of three-dimensional viscous falling films. *J. Fluid Mech.* 242 (1992) 529–549.
13. P. Rosenau, A. Oron and J.M. Hyman, Bounded and unbounded patterns of the Benney equation. *Phys. Fluids A* 4 (1992) 1102–1104.
14. A. Oron and O. Gottlieb, Nonlinear dynamics of temporally excited falling liquid films. *Phys. Fluids* 14 (2002) 2622–2636.
15. B. Scheid, A. Oron, P. Colinet, U. Thiele and J.C. Legros, Nonlinear evolution of non-uniformly heated falling liquid films. *Phys. Fluids* 14 (2002) 4130–4151 (2002). Erratum: *Phys. Fluids* 15 (2003) 583.
16. T.R. Salamon, R.C. Armstrong and R.A. Brown, Traveling waves on vertical films: Numerical analysis using the finite element method. *Phys. Fluids A* 6 (1994) 2202–2220.
17. O. Gottlieb and A. Oron, Stability and bifurcations of parametrically excited thin liquid films. *Int. J. Bifurcation Chaos* (2004) in press.
18. T. Ooshida, Surface equation of falling film flows with moderate Reynolds number and large but finite Weber number. *Phys. Fluids* 11 (1999) 3247–3269.
19. H.-C. Chang, E.A. Demekhin and D.I. Kopelevich, Nonlinear evolution of waves on a vertically falling film. *J. Fluid Mech.* 250 (1993) 433–480.
20. H.-C. Chang, Wave evolution on a falling film. *Ann. Rev. Fluid Mech.* 26 (1994) 103–136.
21. L.T. Nguyen and V. Balakotaiah, Modeling and experimental studies of wave evolution on free falling viscous films. *Phys. Fluids* 12 (2000) 2236–2256.
22. C. Ruyer-Quil and P. Manneville, Improved modeling of flows down inclined planes. *Eur. Phys. J. B* 15 (2000) 357–369.
23. C. Ruyer-Quil and P. Manneville, Further accuracy and convergence results on the modeling of flows down inclined planes by weighted-residual approximations. *Phys. Fluids* 14 (2002) 170–183.
24. V.Ya. Shkadov, Wave flow regimes of a thin layer of a viscous fluid subject to gravity. *Izv. Akad. Nauk SSSR, Mekh. Zhidk. Gaza* 2 (1967) 43–50. Also, translated in *Fluid Dynamics* 2 (1970) 29–34.
25. S.P. Lin, Finite amplitude side-band stability of a viscous film. *J. Fluid Mech.* 63 (1974) 417–429.

26. H.-C. Chang, Onset of nonlinear waves on falling films. *Phys. Fluids A* 1 (1989) 1314–1327.
27. D.R. Lide (ed.), *CRC Handbook of Chemistry and Physics*, 82 Ed. Boca Raton: CRC Press (2001) p. 6–3.
28. C. Ruyer-Quil, personal communication.
29. A. Newell, Envelope equations. In: A. Newell (ed.), *Nonlinear Wave Motion*, Providence, RI: AMS. Lectures in Appl. Math. 15 (1974) pp. 157–163.
30. I.S. Aranson and L. Kramer, The world of the complex Ginzburg-Landau equation. *Rev. Mod. Phys.* 74 (2002) 99–143.
31. B. Scheid, P. Colinet, J.C. Legros, C. Ruyer-Quil and U. Thiele, Validity domain of the Benney's equation including Marangoni effect for closed and open flows. Winter school on *Multi-disciplinary fluid physics of systems with interfaces*, Brussels, February 2003 and preprint.
32. B. Scheid, *Evolution and Stability of Falling Liquid Films with Thermocapillary Effects*. Ph.D. Thesis, Brussels: Université Libre de Bruxelles (2004) 236pp.